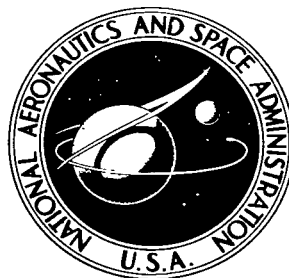


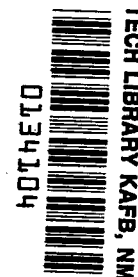
**NASA TECHNICAL NOTE**



**NASA TN D-8370**

*C.I.*

**NASA TN D-8370**




LOAN COPY: RETURN  
AFWL TECHNICAL LIBRARY  
KIRTLAND AFB, N. M.

# PERFORMANCE EVALUATION OF A QUASI-MICROSCOPE FOR PLANETARY LANDERS

*Ernest E. Burcher, Friedrich O. Huck,  
Stephen D. Wall, and Susan B. Woehrle*

*Langley Research Center  
Hampton, Va. 23665*

1. Report No. NASA TN D-8370	2. Government Accession No.	3. 
4. Title and Subtitle PERFORMANCE EVALUATION OF A QUASI-MICROSCOPE FOR PLANETARY LANDERS	5. 0134104 March 1977	6. Performing Organization Code
	8. Performing Organization Report No. L-11162	
7. Author(s) Ernest E. Burcher, Friedrich O. Huck, Stephen D. Wall, and Susan B. Woehrle	10. Work Unit No. 506-18-21-02	11. Contract or Grant No.
9. Performing Organization Name and Address NASA Langley Research Center Hampton, VA 23665	13. Type of Report and Period Covered Technical Note	14. Sponsoring Agency Code
	12. Sponsoring Agency Name and Address National Aeronautics and Space Administration Washington, DC 20546	
15. Supplementary Notes Ernest E. Burcher: Langley Research Center. Friedrich O. Huck: Langley Research Center. Stephen D. Wall: Langley Research Center. Susan B. Woehrle: McDonnell Center for the Space Sciences, Washington University, St. Louis, Missouri 63130.		
16. Abstract  Spatial resolutions achieved with cameras on lunar and planetary landers have been limited to about 1 mm, whereas microscopes of the type proposed for such landers could have obtained resolutions of about 1 $\mu$ m but were never accepted because of their complexity and weight. The quasi-microscope evaluated in this paper could provide intermediate resolutions of about 10 $\mu$ m with relatively simple optics that would augment a camera, such as the Viking lander camera, without imposing special design requirements on the camera or limiting its field of view of the terrain. Images of natural particulate samples taken in black and white and in color have shown that grain size, shape, and texture are made visible for unconsolidated materials in a 50- to 500- $\mu$ m size range. Such information may provide broad outlines of planetary surface mineralogy and allow inferences to be made of grain origin and evolution. The mineralogical descriptions of single grains would be aided by the reflectance spectra that could, for example, be estimated from the six-channel multispectral data of the Viking lander camera.		
17. Key Words (Suggested by Author(s))  Optics Imaging Planetary missions	18. Distribution Statement  Unclassified - Unlimited  Subject Category 35	
19. Security Classif. (of this report) Unclassified	20. Security Classif. (of this page) Unclassified	21. No. of Pages 23
		22. Price* \$3.25

# PERFORMANCE EVALUATION OF A QUASI-MICROSCOPE

## FOR PLANETARY LANDERS

Ernest E. Burcher, Friedrich O. Huck, Stephen D. Wall,  
and Susan B. Woehrle\*  
Langley Research Center

### SUMMARY

Spatial resolutions achieved with cameras on lunar and planetary landers have been limited to about 1 mm, whereas microscopes of the type proposed for such landers could have obtained resolutions of about 1  $\mu\text{m}$  but were never accepted because of their complexity and weight. The quasi-microscope evaluated in this paper could provide intermediate resolutions of about 10  $\mu\text{m}$  with relatively simple optics that would augment a camera, such as the Viking lander camera, without imposing special design requirements on the camera or limiting its field of view of the terrain. Images of natural particulate samples taken in black and white and in color have shown that grain size, shape, and texture are made visible for unconsolidated materials in a 50- to 500- $\mu\text{m}$  size range. Such information may provide broad outlines of planetary surface mineralogy and allow inferences to be made of grain origin and evolution. The mineralogical descriptions of single grains would be aided by the reflectance spectra that could, for example, be estimated from the six-channel multispectral data of the Viking lander camera.

### INTRODUCTION

Visual imaging is generally accepted to be of primary importance in exploring the Moon and the planets by landed spacecraft, as has been demonstrated by the USSR Luna (ref. 1), Lunakhod (ref. 2), Venera (refs. 3 to 5), U.S. Surveyor (ref. 6), and Viking (ref. 7) missions. Surface resolutions that could be obtained with the imaging systems on these spacecraft have been limited to about 1 to 10 mm. Substantial improvements in resolution could be achieved by the use of automatic focusing techniques; however, such techniques would substantially increase the complexity of the imaging system (ref. 8). Microscopes with resolutions down to 0.4  $\mu\text{m}$  have also been proposed (refs. 9 to 11), but have never been accepted for a space mission, partly because of their complexity, weight, and cost. They require elaborate mechanisms for sample preparation and special imaging systems with precise focus control.

A quasi-microscope concept was introduced and analyzed in references 12 and 13 to bridge the gap between the resolutions obtainable with planetary lander cameras and the much higher resolutions obtainable only with complex

---

\*McDonnell Center for the Space Sciences, Washington University, St. Louis, Missouri 63130.

microscopes. A quasi-microscope consists of a planetary lander camera augmented with auxiliary optics that do not impose special design requirements on the camera or limit its normal function to image the surrounding terrain. Evaluations of this concept are essentially limited to the Viking lander camera (ref. 14). The camera has an instantaneous field of view of  $0.12^\circ$  for multispectral imaging with six spectral channels in the 0.4- to 1.0- $\mu\text{m}$  wavelength range, and an instantaneous field of view of  $0.04^\circ$  for broadband imaging with four electronically selectable focus steps. The depth of field extends from 1.7 m to infinity, and the smallest detail that can be resolved is about 1.5 mm (ref. 15).

First-order optical analyses indicate that the use of a single lens as magnifier could yield a resolution of about 40  $\mu\text{m}$ , with a depth of field of 500  $\mu\text{m}$  for each focal position and an unvignetted object-area diameter of 6 mm (that is, 150 picture elements) (ref. 12). Analyses of a more complex auxiliary optical system consisting of a field lens in addition to the magnifier indicated that a tenfold improvement could be obtained in resolution, that is, about 4  $\mu\text{m}$ . The corresponding depth of field would be 11  $\mu\text{m}$  at each focal position and the unvignetted object-area diameter would be 1 to 1.6 mm (that is, 250 to 400 picture elements), depending on the size of the field lens (ref. 13). Preliminary design trade-off analyses by the Perkin-Elmer Corporation (under NASA contract) led to the selection of an optical system that could provide a resolution of 11  $\mu\text{m}$  as a favorable compromise between performance capability and design complexity. The corresponding depth of field was predicted to be 32  $\mu\text{m}$  for each focal position (that is, 128  $\mu\text{m}$  with four focus steps) and the unvignetted object-area diameter to be 4 mm (that is, 372 picture elements). A relay lens was also added to limit the size of the field lens that would otherwise be required to obtain this object area.

The quasi-microscope design could be further refined, especially with regard to the total number and thicknesses of lens elements. However, it appeared prudent to implement the preliminary design and to evaluate the overall performance. The evaluation is divided into two parts: (1) an optical performance analysis including resolution, depth of field, and field of view, and (2) an analysis of the quality and kinds of information that are provided about the physical and chemical characteristics of regolith material.

#### SYMBOLS

D	lens diameter, $\mu\text{m}$
d	diameter of picture element (pixel) or resolution diameter, $\mu\text{m}$
F	F-number or $f/D$
f	focal length, m
lp/mm	line pairs per mm
$\ell$	object or image distance from lens, m

$\Delta l$	depth of field or focus, m
m	transverse magnification
$\lambda$	wavelength, $\mu\text{m}$
$\Omega$	number of unvignetted picture elements (pixels) in central line scan

Subscripts:

c	camera lens
f	field lens
o	objective lens
r	relay lens

Primes denote image space.

#### SYSTEM DESCRIPTION

Figure 1 presents a simplified cutaway view of the Viking lander camera augmented with the quasi-microscope optics. The material to be viewed is inserted in the slot under the optics, in one of several possible ways. Perhaps the simplest way would be to use a small turntable as follows: A surface sampler, such as the one on the Viking lander, could deposit some material on one side of the turntable, and the turntable could then be rotated to bring the sample under the quasi-microscope optics. As the sample is rotated, it would pass under a leveling arm which would smooth the sample to a thin layer compatible with the optical depth of field of the quasi-microscope. After the sample has been viewed, the turntable could be rotated several times until a brush has cleaned off the sample.

The camera is basically a radiometer with an optical-mechanical scanning mechanism. It features an array of 12 silicon photodiodes, consisting of 4 broadband channels with selectable focus for high-resolution imaging, 1 broadband channel for rapid surveys, 6 narrowband channels for color and near-infrared multispectral imaging, and 1 narrowband channel for scanning the Sun. The instantaneous fields of view are  $0.04^\circ$  for the four high-resolution channels and  $0.12^\circ$  for the other channels. A nodding mirror scans the instantaneous fields of view in elevation from  $40^\circ$  above to  $60^\circ$  below the plane normal to the optical axis, and the upper housing rotates in azimuth between successive line scans with selectable frame widths ranging from  $2.5^\circ$  up to  $342.5^\circ$ . Light falling on the selected photodiode is transduced into an electrical signal which is amplified, sampled, and quantized for digital transmission. Table I presents a summary of pertinent design and performance characteristics.

The narrow window of the camera usually hides behind a post to avoid unnecessary exposure to dust. The dust post would have to be slightly enlarged to contain the quasi-microscope. The auxiliary optics could thus be within view

of the camera without appreciably limiting the camera's field of view of the surrounding terrain. The present dust post limits the field of view by  $17.5^\circ$ ; the enlarged dust post would limit it by  $29^\circ$ .

Figure 2(a) presents a detailed drawing of camera and quasi-microscope optics, and figure 2(b) is a thin-lens representation. The objective lens focuses a magnified image of the sample onto a negative field lens, and the relay lens presents this image in the form of (nearly) parallel light rays to the camera. The camera scans this image with a photosensor focused at (nearly) infinity. The distance between the camera and quasi-microscope is not critical for focus; however, the useful field of view will decrease due to vignetting if the distance between the scanning mirror and quasi-microscope relay lens is appreciably increased.

Figure 3 presents a simplified thin-lens representation of the optics together with performance equations based on first-order geometric analyses. (See ref. 13.) Performance predictions that result from substituting proper values into these equations are summarized in table II.

## SYSTEM EVALUATION

### Optical Performance

Any line-scan camera such as the Viking lander camera is basically an optical sampling system with a spatial frequency response which, unlike the time frequency responses of electronics, is difficult to shape. It is important to divorce the image quality degradation that is imposed by optical performance limitations of the system from the additional degradation that is introduced if spatial detail is undersampled. That is, the angular resolution of the camera is unavoidably limited by the trade-off required between camera instantaneous field of view, sensitivity, and depth of field (refs. 6 and 12), whereas the sampling interval can be somewhat independently selected (refs. 16 to 19). It is, therefore, advantageous to evaluate the quasi-microscope with a laboratory facsimile camera that features a variable sampling interval in addition to a camera lens and photosensor aperture that are identical to those of the Viking lander camera.

Figure 4 shows a test setup of the laboratory facsimile camera augmented with the quasi-microscope. Unless otherwise specified, all resolution measurements were made with a high-resolution ( $0.04^\circ$ ) photosensor aperture and (nearly) sufficient sampling intervals ( $0.02^\circ$ ).

Resolution capability is generally best specified as sine-wave modulation transfer function (MTF). Since sine-wave targets were not available, square-wave or tribar targets are the next best alternative. Therefore, the National Bureau of Standards (NBS) resolution test chart shown in figure 5 was selected. When photographically reduced to 7.5, the chart provides tribars ranging from 3.5 to 24 lp/mm, and when reduced by 25, tribars range from 12 to 83 lp/mm; thus, the range of spatial frequencies of interest is adequately covered.

Figure 6 presents an average curve of several tribar frequency response measurements. The limiting resolution is about  $11\ \mu\text{m}$  (that is,  $22\ \mu\text{m}/\text{lp}$  or  $45\ \text{lp}/\text{mm}$ ), which is in close agreement with the first-order optical analysis prediction summarized in table II. The resolution is primarily limited by the photosensor aperture size rather than by quasi-microscope blurring or by camera sampling, as indicated by the three pictures of the NBS chart shown in figure 7. Figures 7(a) and 7(b), which were obtained with the facsimile camera at sampling intervals of  $0.04^\circ$  and  $0.02^\circ$ , respectively, show that sampling intervals broader than  $0.02^\circ$  reduce image quality. Figure 7(c), which was obtained with a film camera with optics similar to those of the facsimile camera, shows that improvements in the angular resolution of the camera will lead to higher spatial resolutions with the quasi-microscope.

The usable object area (that is, quasi-microscopic field of view) was determined by counting the number of unvignetted pixels (about 360) along a diameter of a computer printout of the image, and multiplying this number by the diameter of a pixel in the object field (that is, by  $11\ \mu\text{m}$ ). The resulting diameter is about  $4\ \text{mm}$ , which is again in close agreement with the predictions listed in table II.

Two square-wave targets were used to measure the spatial frequency response as a function of defocus (that is, quasi-microscopic depth of field) at  $25\ \text{lp}/\text{mm}$  ( $40\ \mu\text{m}/\text{lp}$ ) and  $40\ \text{lp}/\text{mm}$  ( $25\ \mu\text{m}/\text{lp}$ ). The targets were mounted at a  $6^\circ$  slope to cover a depth of  $0.4\ \text{mm}$  over the  $4\text{-mm}$ -diameter area. Figure 8 presents plots of the square-wave spatial frequency response against distance from the in-focus plane. These results indicate that the square-wave response for  $40\ \text{lp}/\text{mm}$  detail remains above 5 percent over a depth of field of about  $0.13\ \text{mm}$  per focus step, and for  $25\ \text{lp}/\text{mm}$  over a depth of field of about  $0.32\ \text{mm}$ . The useful depth of field of the quasi-microscope is thus appreciably larger for detail slightly above the quasi-microscope resolution limit than the geometric depth of field prediction. (See table II.)

The resolution could be increased with a quasi-microscope designed for higher magnification, but only at the expense of a decreased object field and/or an increased optical complexity. A more attractive approach to increase resolution would be through an increase in the angular resolution of the camera. An increase in angular camera resolution by a certain factor (up to about 3) would increase the resolution obtained with the quasi-microscope by nearly the same factor, whereas the object field would remain the same. (See refs. 12 and 13.)

The relative spectral transmittance was determined as the ratio of the spectral radiance of a lamp imaged directly to that of the lamp imaged through the quasi-microscope onto the entrance slit of a monochromator. The measurements were made at  $0.05\text{-}\mu\text{m}$  intervals over the wavelength range  $0.4$  to  $1.1\ \mu\text{m}$  by using a filter to block the second-order dispersions of the monochromator grating. The absolute transmittance was measured at a single wavelength ( $0.9\ \mu\text{m}$ ) as the ratio of the signal measured directly with a collimated light beam to the signal for the light beam through the quasi-microscope. The resultant absolute spectral transmittance curve is plotted in figure 9.

## Mineralogical Analysis

The quasi-microscope provides a new tool for planetary exploration, both for identification and for examination of constituent materials composing planetary regoliths, with resolutions normally obtained only in the laboratory. The analysis presented in this paper is limited to the range and quality of information that could be obtained about the inorganic characteristics of regolith material, although the concept may also have biological applications.

Figure 10 presents black and white images of five geologic materials. The samples and their composition are summarized in table III. The images were obtained with the camera  $0.04^\circ$  instantaneous field of view, by using insufficient ( $0.04^\circ$ ) and nearly sufficient ( $0.02^\circ$ ) sampling intervals. The images show that small details are better resolved with nearly sufficient sampling, and that the increased data required should generally be worthwhile. Figure 11 presents color images of three of the five materials. The images were obtained with the  $0.12^\circ$  instantaneous field of view and (nearly) sufficient ( $0.06^\circ$ ) sampling intervals. Information about grain sizes, shapes, and colors that can be extracted from these images provides clues about (1) the size distribution of grains produced by igneous (intrusive and extrusive) processes or by shock metamorphism; (2) the size distribution resulting from sorting and abrasion during transport by wind, water, or ballistic processes; (3) constituent mineral components deduced from cleavage and fracture patterns; (4) the degree of chemical and physical alteration deduced from the degree of roundness and grain sphericity; and (5) an estimate of mineralogic composition obtained by an examination of color. For instance, grain morphologies and textures of the material in figure 10 are well defined. The labradorite can be distinguished by its high reflectance and pattern of cleavage from the two pyroxenes, augite and hypersthene. The two pyroxenes, which comprise the dark grains, are difficult to distinguish by their morphology and texture alone. The color image (fig. 11(a)), however, permits augite and hypersthene to be more readily distinguished, the augite as golden green, and the hypersthene as reddish brown.

The highly irregular and rounded surfaces of the material in figure 10(b) tentatively identify it as a highly altered material. Aggregated grains and pitted surface textures tend to support this conclusion. The reddish-brown color of the sample (fig. 7(b)) aids to define the sample as limonite or goethite.

The fine grained and dark material in figure 10(c) can perhaps be recognized as the presence of a large percentage of mafic minerals, like pyroxene and olivine. Only minor amounts of a lighter mineral, such as feldspar, are observed. This is a close approximation to the composition of this sample, a peridotite. Again, as with the morite sample, color images (fig. 11) would help to distinguish between the mafic minerals.

The materials in figures 10(d) and 10(e) are difficult to distinguish, although they have dramatically different mineralogies. Both samples appear to consist of rounded bright grains, but those in figure 10(d) are feldspar constituents of a latite, and those in figure 10(e) are quartz constituents of a volcanic tuff breccia. Perhaps the only distinguishing characteristic is the



higher brightness of the quartz grains. This problem of identification is not easily solved, and color images alone would not entirely clarify the difference.

The problem of unique identification of sample mineralogy could be partially circumvented by utilizing the Viking lander camera's six-channel multi-spectral capability to produce single particle reflectivity spectra (ref. 20). The present capability extends from 0.4 to 1.1  $\mu\text{m}$ , and has the potential to provide important information about the presence of transition metals (Fe, Ti, and Cr) and the nature of their valence states and bonding character in silicates, oxides, and hydroxides. (See ref. 17.) Such single crystal spectra, for instance, would allow one to distinguish between hypersthene, augite, and Fe-bearing olivine, since the distinctive  $\text{Fe}^{+2}$  transition absorption band characteristically shifts from 0.85  $\mu\text{m}$  (hypersthene) to 0.95  $\mu\text{m}$  (augite) to 1.03 to 1.05  $\mu\text{m}$  (olivine). The possible extension of the Viking lander camera's spectral range to 2.5  $\mu\text{m}$  by use of PbS detectors would greatly enhance this capability.

#### CONCLUDING REMARKS

The preliminary quasi-microscope design that was evaluated in this paper consists of a five-element objective lens, a one-element field lens, and a six-element relay lens. The optics fit into a slightly enlarged dust post of the Viking lander camera without appreciably limiting the camera field of view of the terrain.

The quasi-microscope can provide a resolution of nearly 10  $\mu\text{m}$  over a 4-mm-diameter area if the object is in exact focus. The effective depth of field is about 0.13 mm for 25  $\mu\text{m}/\text{lp}$  detail and 0.32 mm for 40  $\mu\text{m}/\text{lp}$  detail. Increased resolution could be obtained with higher quasi-microscope magnification at the expense of a decreased object field and/or an increased optical complexity. The resolution is primarily limited by the photosensor aperture of the camera; an increase in the angular resolution of the camera up to a factor of three would provide a corresponding increase in quasi-microscope resolution without decreasing the object area.

The optical resolutions possible with the quasi-microscope are normally obtained only in the laboratory. By utilizing multispectral techniques with high resolution monospectral imagery, a great deal of information can be obtained about regolith origin and modification by physical or chemical processes. Much of the important analysis done at the Lunar Receiving Laboratory at Lyndon B. Johnson Space Center involved microscopic analysis of soils; much of that type of analysis could be accomplished by including a quasi-microscope on the next planetary lander.

Langley Research Center  
National Aeronautics and Space Administration  
Hampton, VA 23665  
November 9, 1976

## REFERENCES

1. Selivanov, A. S.; Govorov, V. M.; Titov, A. S.; and Chemodanov, V. P.: Lunar Station Television Camera. Contract NAS 7-100, Reilly Translations, 1968. (Available as NASA CR-97884.)
2. Selivanov, A. S.; Govorov, V. M.; Zasetskii, V. V.; and Timokhin, V. A. (Morris D. Friedman, transl.): Chapter V. Peculiarities of the Construction and Fundamental Parameters of the "Lunokhod-1" Television Systems. Lockheed Missiles & Space Co. Transl. (From Peredvizhenaiia Laboratoriia na Lune - Lunokhod-1, Acad. Sci. SSSR Press (Moscow), 1971, pp. 55-64.)
3. First Venus Photo Returned by Venera-9. Aviat. Week & Space Technol., vol. 103, no. 17, Oct. 27, 1975, p. 15.
4. Brown, David A.: Data Show Venus Young Evolving Planet. Aviation Week & Space Technol., vol. 103, no. 18, Nov. 3, 1975, pp. 19-20.
5. Soviet Venera Instrumentation Detailed. Aviation Week & Space Technol., vol. 103, no. 20, Nov. 17, 1975, p. 52.
6. Surveyor Project Staff: Surveyor Project Final Report. Pt. I: Project Description and Performance - Volume I. Tech. Rep. 32-1265, Jet Propulsion Lab., California Inst. Technol., July 1, 1969. (Available as NASA CR-105302.)
7. Mutch, T. A.; Binder, A. B.; Huck, F. O.; Levinthal, E. C.; Morris, E. C.; Sagan, Carl; and Young, A. T.: Imaging Experiment: The Viking Lander. Icarus, vol. 16, no. 1, Feb. 1972, pp. 92-110.
8. Huck, Friedrich O.; and Lambiotte, Jules J., Jr.: A Performance Analysis of the Optical-Mechanical Scanner as an Imaging System for Planetary Landers. NASA TN D-5552, 1969.
9. Greene, V. W.; Landgren, D. A.; Mullin, D. D.; and Peterson, R. E.: Microscopic System for Mars Study Program. Rep. No. 2326 (JPL Contract 950123), Electron Div., Gen. Mills, Inc., August 30, 1962. (Available as NASA CR-51538.)
10. Loomis, Alden A.: A Lunar and Planetary Petrography Experiment. Tech. Rep. No. 32-785, Jet Propulsion Lab., California Inst. Technol., Sept. 1, 1965. (Available as NASA CR-64917.)
11. Soffen, Gerald A.: Extraterrestrial Optical Microscopy. Appl. Opt., vol. 8, no. 7, July 1969, pp. 1341-1348.
12. Huck, Friedrich O.; Sinclair, Archibald R.; and Burcher, Ernest E.: First-Order Optical Analysis of a Quasi-Microscope for Planetary Landers. NASA TN D-7129, 1973.

13. Wall, Stephen D.; Burcher, Ernest E.; and Huck, Friedrich O.: Optical Analysis of a Compound Quasi-Microscope for Planetary Landers. NASA TN D-7414, 1974.
14. Huck, F. O.; McCall, H. F.; Patterson, W. R.; and Taylor, G. R.: The Viking Mars Lander Camera. Space Science Instrum., vol. 1, no. 2, May 1975, pp. 189-241.
15. Huck, F. O.; and Wall, S. D.: Image Quality Prediction: An Aid to the Viking Lander Imaging Investigation on Mars. Appl. Opt., vol. 15, no. 7, July 1976, pp. 1748-1766.
16. Katzberg, Stephen J.; Huck, Friedrich O.; and Wall, Stephen D.: Photo-sensor Aperture Shaping To Reduce Aliasing in Optical-Mechanical Line-Scan Imaging Systems. Appl. Optics, vol. 12, no. 5, May 1973, pp. 1054-1060.
17. Huck, Friedrich O.; and Park, Stephen K.: Formulation of the Information Capacity of the Optical-Mechanical Line Scan Imaging Process. NASA TN D-7942, 1975.
18. Huck, Friedrich O.; and Park, Stephen K.: Optical-Mechanical Line-Scan Imaging Process: Its Information Capacity and Efficiency. Appl. Opt., vol. 14, no. 10, Oct. 1975, pp. 2508-2520.
19. Biberman, Lucien M., ed.: Perception of Displayed Information. Plenum Press, Inc., c.1973.
20. Park, Stephen K.; and Huck, Friedrich O.: A Spectral-Reflectance Estimation Technique Using Multispectral Data From the Viking Lander Camera. NASA TN D-8292, 1976.

TABLE I.- PERFORMANCE AND DESIGN CHARACTERISTICS OF VIKING LANDER CAMERA

Characteristics	Survey	Color and infrared	High resolution
Instantaneous field of view, deg	0.12	0.12	0.04
Frame width, deg			
Elevation	61.44	61.44	20.48
Azimuth: min	2.5	2.5	2.5
max	342.5	342.5	342.5
Field of view, deg			
Elevation	100; from 40 above to 60° below horizon, selectable in 10° increments		
Azimuth	342.5; in multiples of 2.5° steps		
Photosensor			
Aperture diameter, $d_c$ , mm	0.12	0.12	0.040
Distance from lens, $l'_c$ , mm	54.5	54.5	55.3, 54.8, 54.4, 53.9
Geometric depth of focus, $\Delta l_c$ , mm	1.38	1.38	0.47, 0.46, 0.46, 0.45
In-focus object distance, $l_c$ , m	3.7	3.7	1.9, 2.7, 4.5, 13.3
Geometric depth of field, $\Delta l_c$ , m	1.7 to $\infty$	1.7 to $\infty$	1.7 to $\infty$
Picture elements per line, $\Omega$	512	512	512
Bits per picture element	6	6	6

TABLE II.- PREDICTED QUASI-MICROSCOPE PERFORMANCE BASED ON  
FIRST-ORDER OPTICAL ANALYSES

Performance parameter	Camera imaging mode	
	High-resolution	Multispectral
Diameter of pixel in object field, $d_o$ , $\mu\text{m}$	11	33
Geometric resolution, $\mu\text{m}/\text{lp}$ (lp/mm)	22 (45)	66 (15)
Geometric depth of field, $\Delta l_o$ , $\mu\text{m}$	32 per focus step or 128 with four focus steps	96
Diameter of unvignetted object field, mm	4.1	4.1
Number of adjacent contiguous pixels per object field diameter, $\Omega$	372	124

TABLE III.- SUMMARY OF GEOLOGIC MATERIALS

Figure	Sample designation	Mineralogic composition
10(a), 11(a)	Norite	Mixture of 1/3 labradorite, 1/3 augite, 1/3 hypersthene, crushed
10(b), 11(b)	Limonite	≈90% limonite, crushed
10(c), 11(c)	Peridotite	≈80% augite, minor olivine and hypersthene; crushed
10(d)	Latite	Plagioclase plus potassium feldspar, minor mafics; crushed
10(e)	Tuff Breccia	Quartz sand and minor feldspar, from Pinacates volcanic field, Mexico

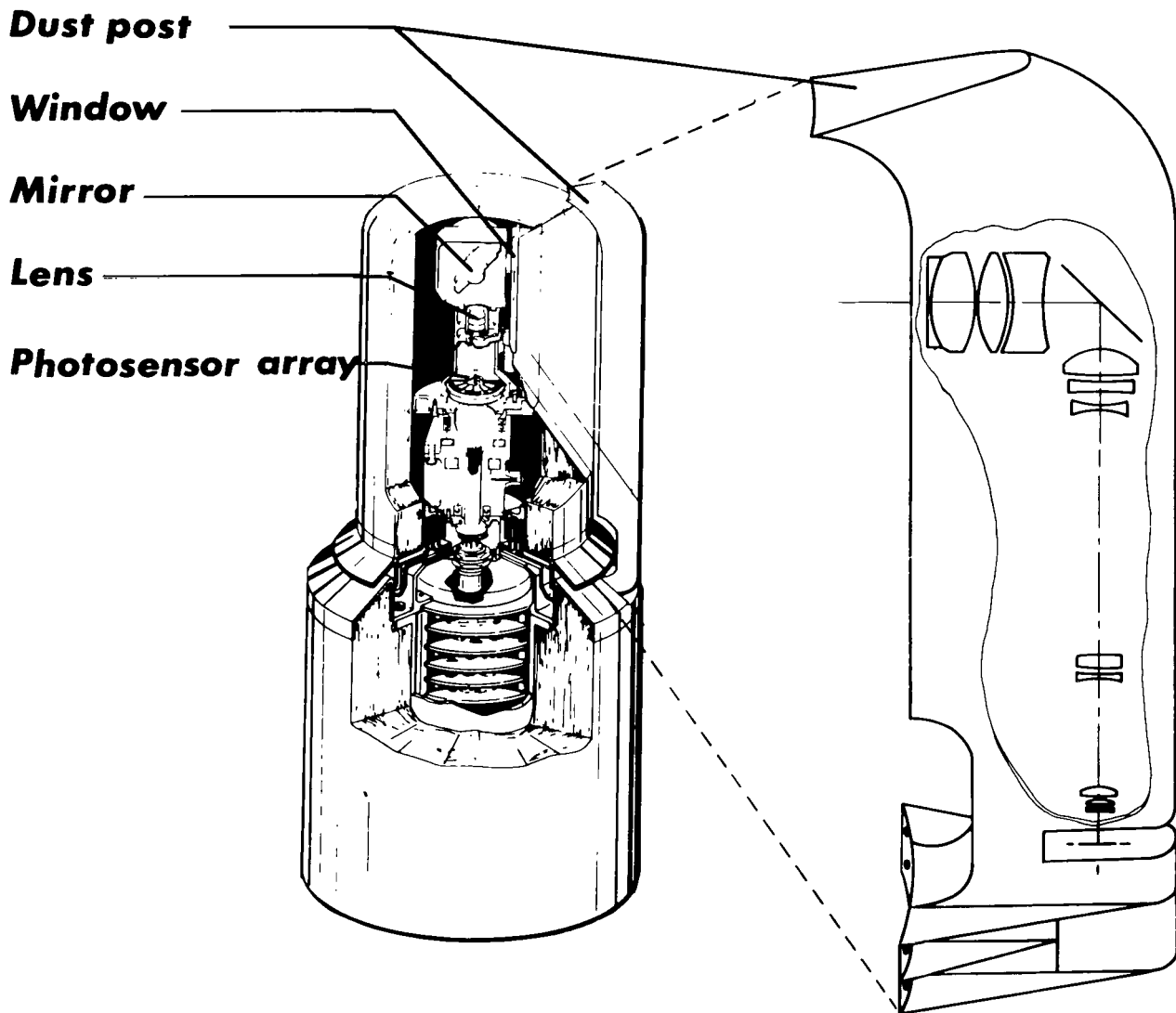
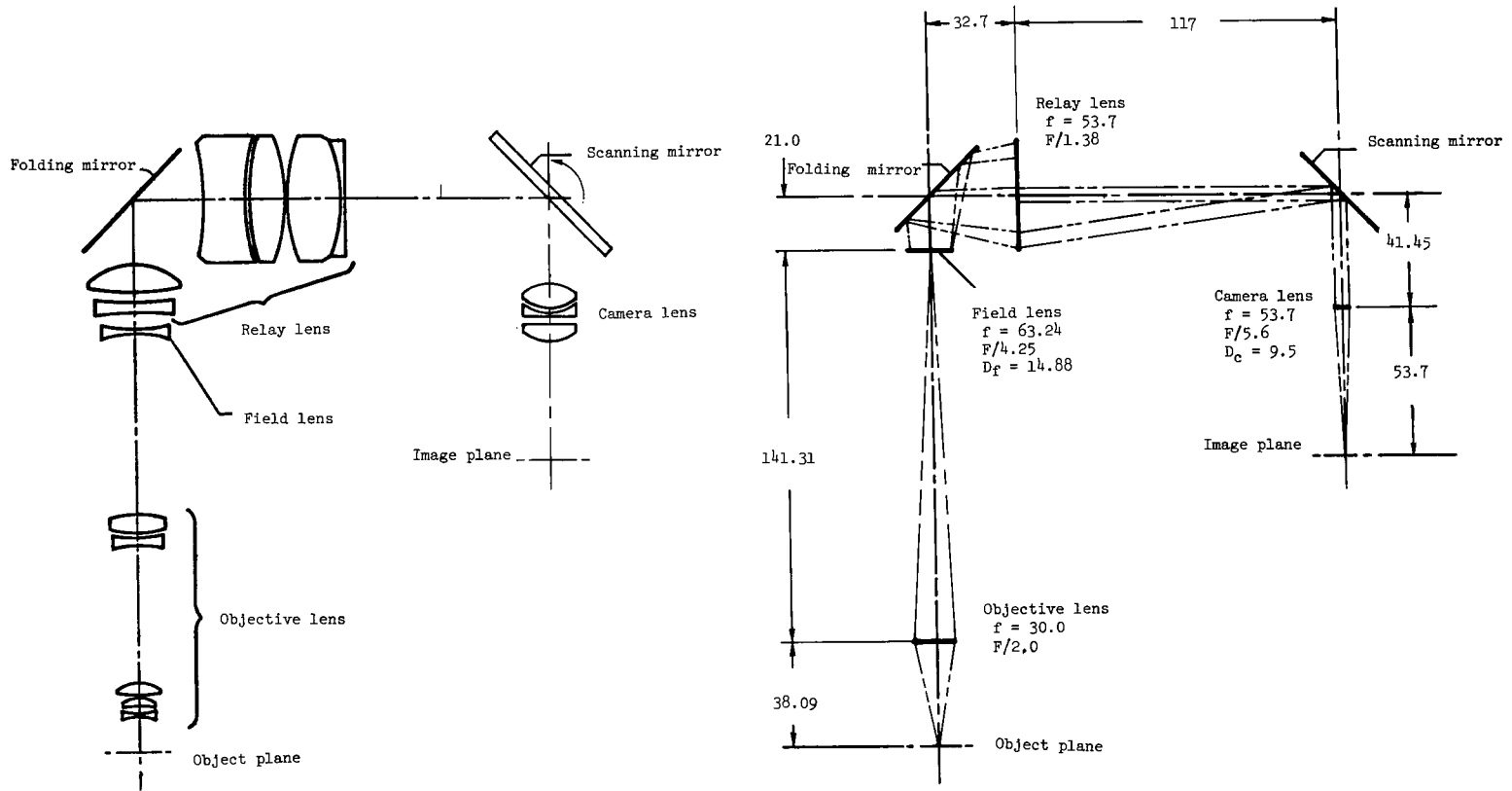


Figure 1.- Simplified cutaway view of Viking lander camera with quasi-microscope optics.

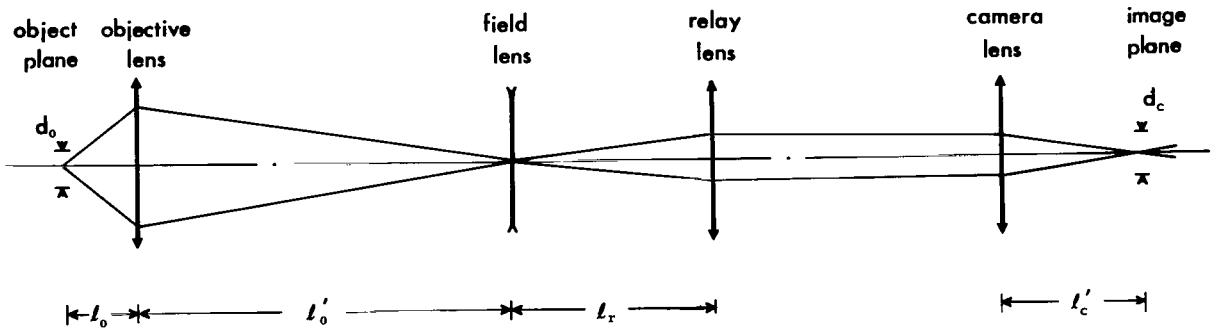


(a) Detail.

(b) Thin-lens representation.

Figure 2.- Camera and quasi-microscope optics. (All dimensions are in mm.)





- TRANSVERSE MAGNIFICATION:

$$m = m_o m_{rc} = \frac{l'_o l'_c}{l_o l_r}$$

THE FOCAL LENGTH OF THE RELAY LENS IS SELECTED TO BE EQUAL TO THAT OF THE CAMERA LENS; HENCE,  $l_r \approx l'_c$

- RESOLUTION:

$$d_o = \frac{d_c}{m}$$

- GEOMETRIC DEPTH OF FIELD:

$$\Delta l_o = \frac{\Delta l_c}{m^2}$$

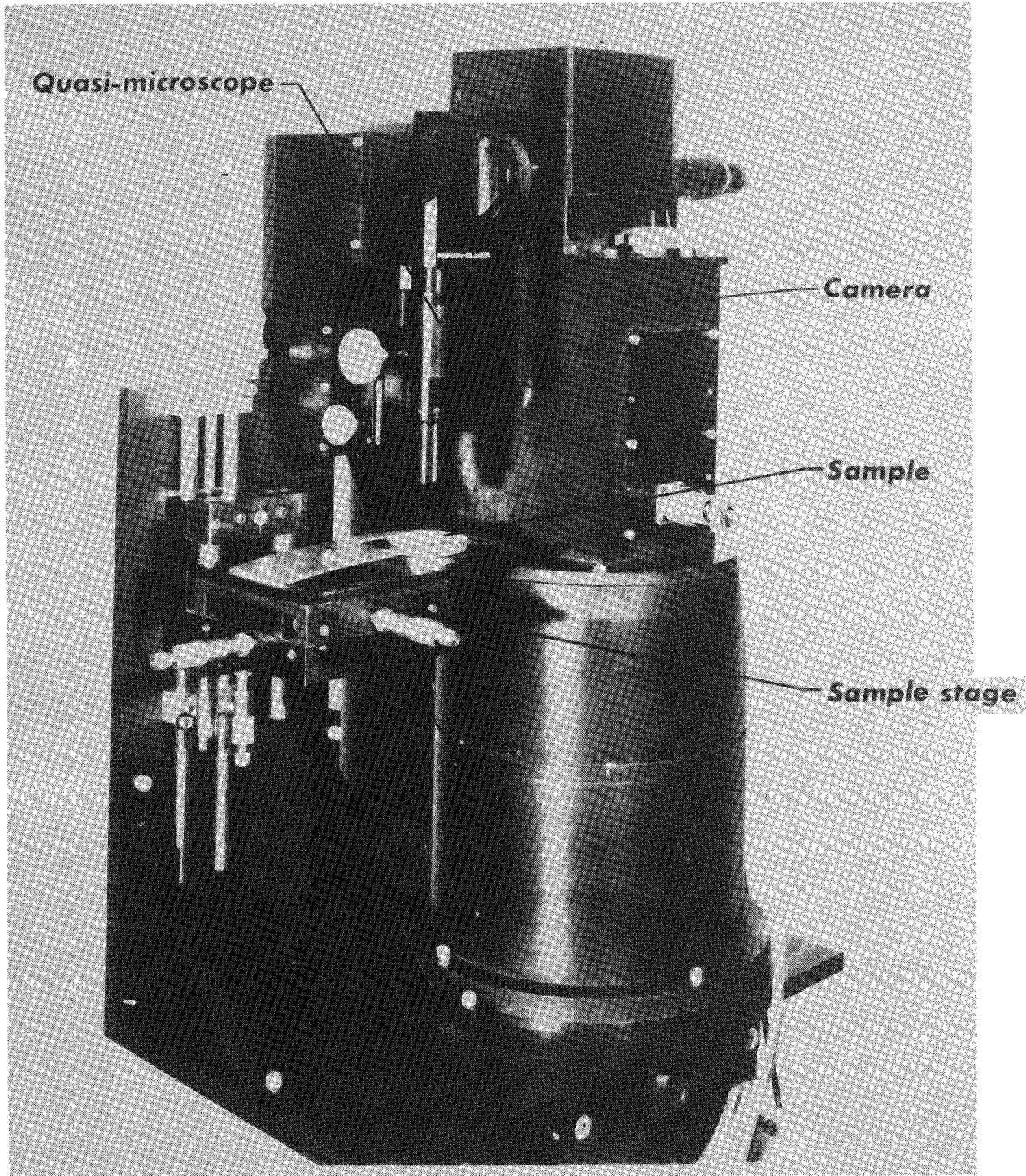
WHERE  $l_c$  IS THE DEPTH OF FOCUS IN THE CAMERA IMAGE PLANE GIVEN BY

$$\Delta l_c = \frac{2l'_c d_c}{D_c}$$

- NUMBER OF ADJACENT UNVIGNETTED PIXELS PER LINE SCAN THROUGH CENTER OF OBJECT:

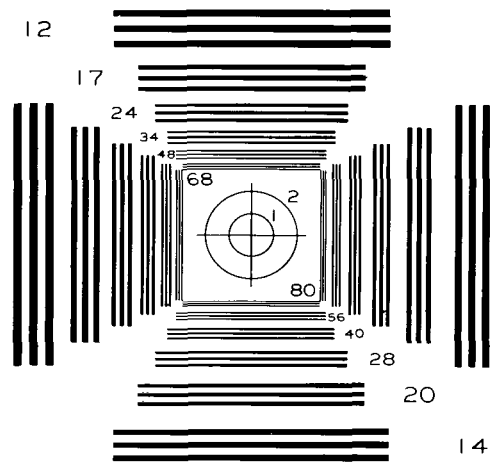
$$\Omega = \frac{D_i l'_c}{l_r d_c}$$

Figure 3.- Thin-lens representation of camera and quasi-microscope optics with performance equations based on first-order geometric analysis (from ref. 13).



L-76-2425.1

Figure 4.- Laboratory facsimile camera with quasi-microscope.



  
 RESOLUTION TEST CHART 1952

Figure 5.- NBS resolution test chart.

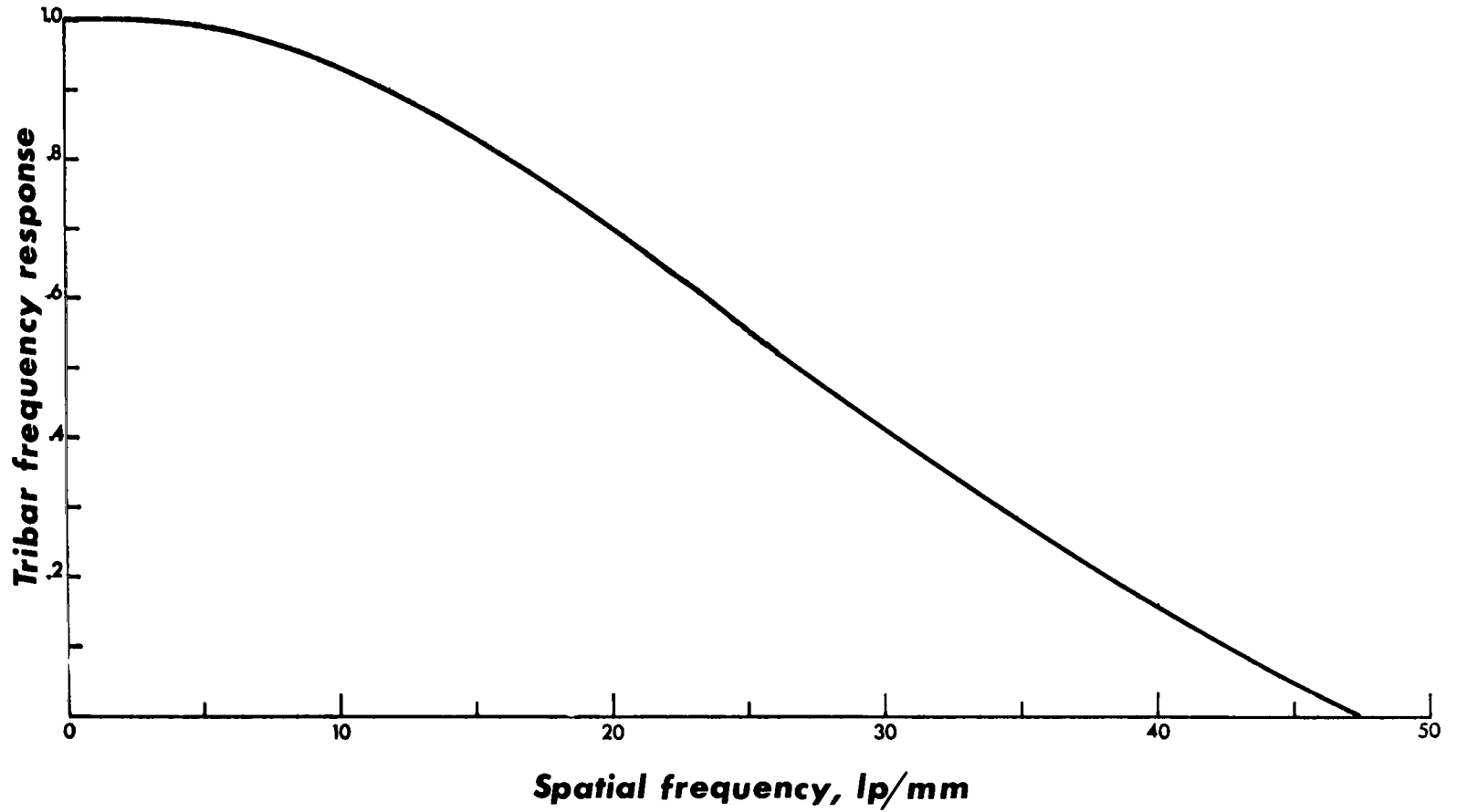
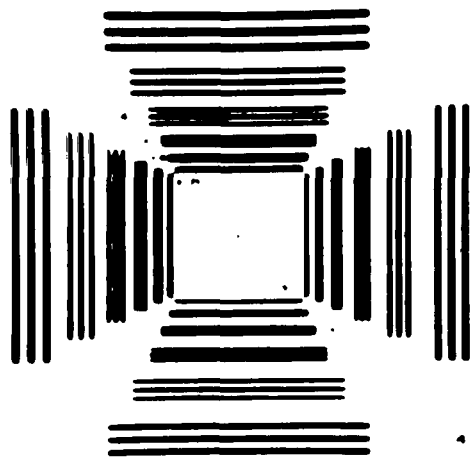
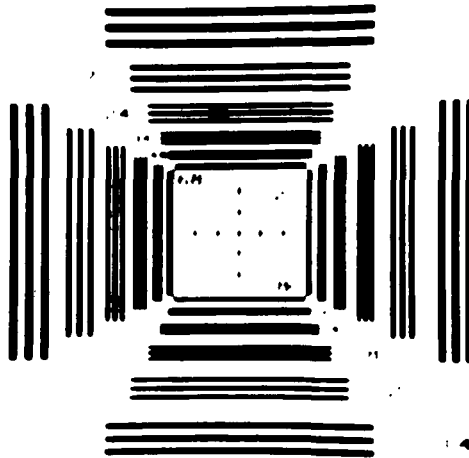


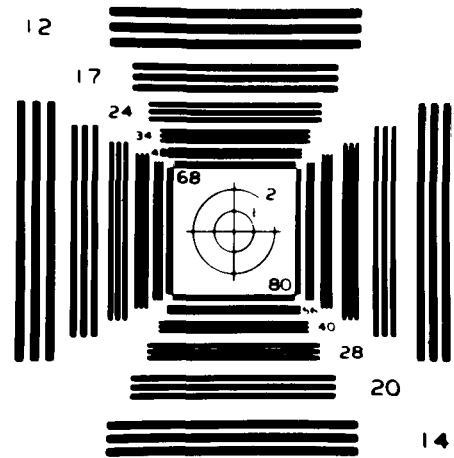
Figure 6.- Tribar frequency response of quasi-microscope and camera.



(a) Laboratory facsimile camera with  $0.04^\circ$  sampling intervals.



(b) Laboratory facsimile camera with  $0.02^\circ$  sampling intervals.



(c) Film camera.

Figure 7.- Images of NBS resolution test chart obtained with the quasi-microscope.

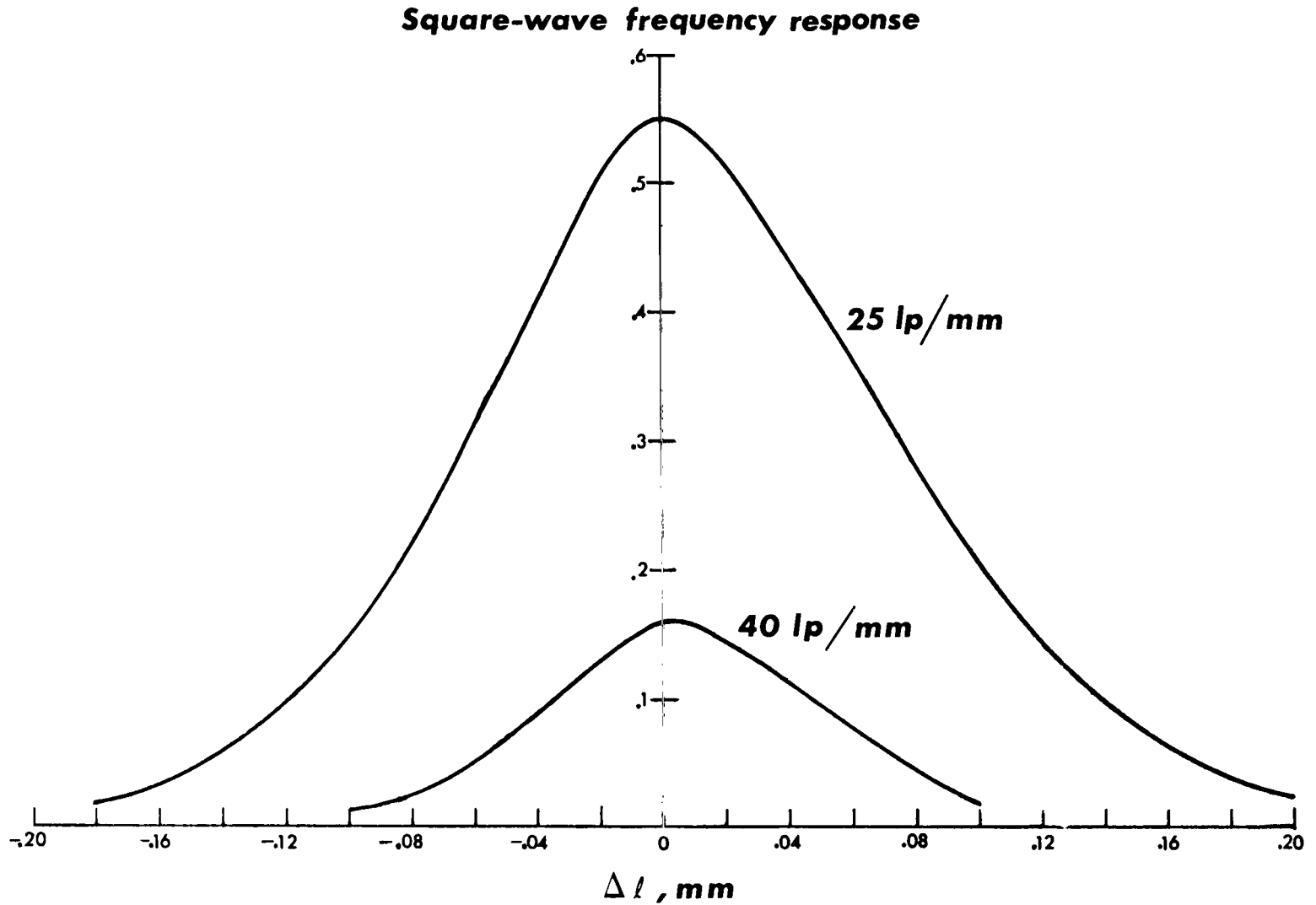


Figure 8.- Square-wave spatial frequency response as function of object distance from focal plane.

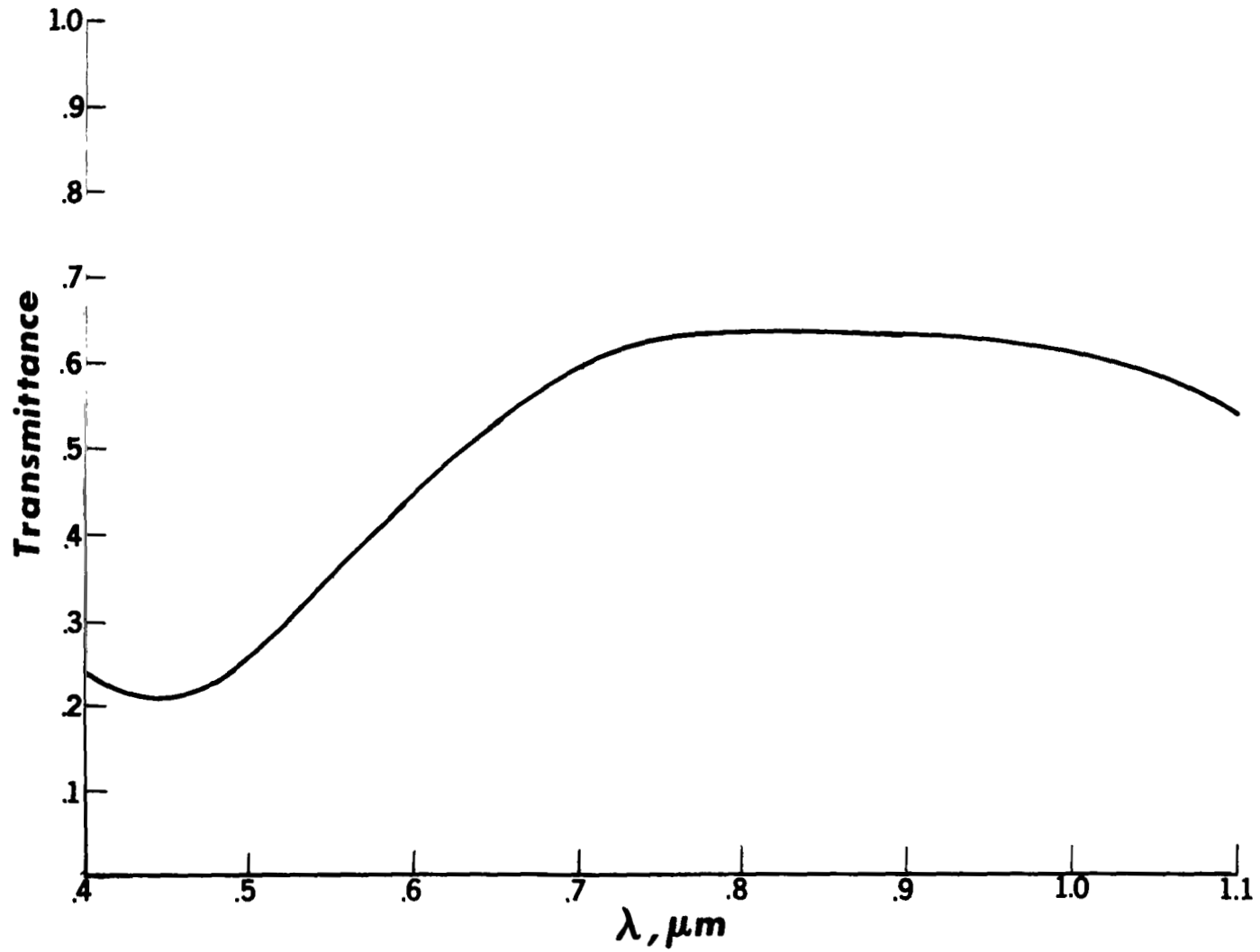
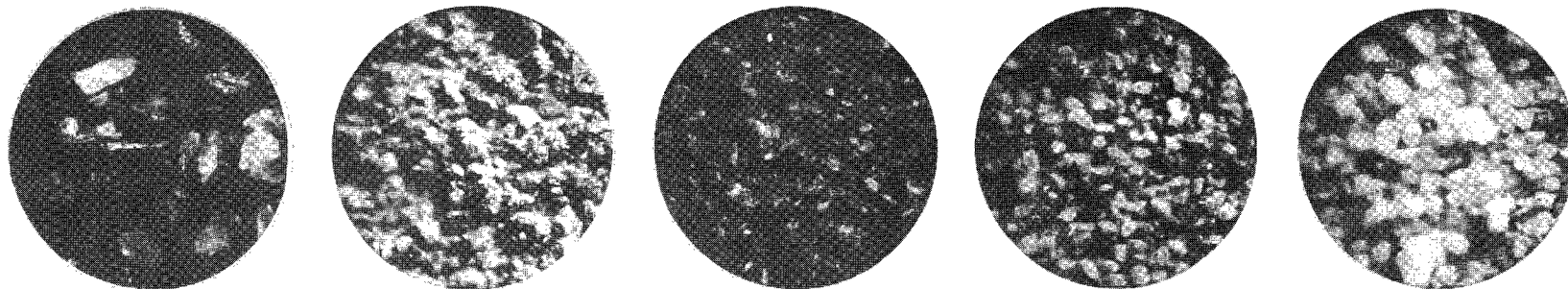
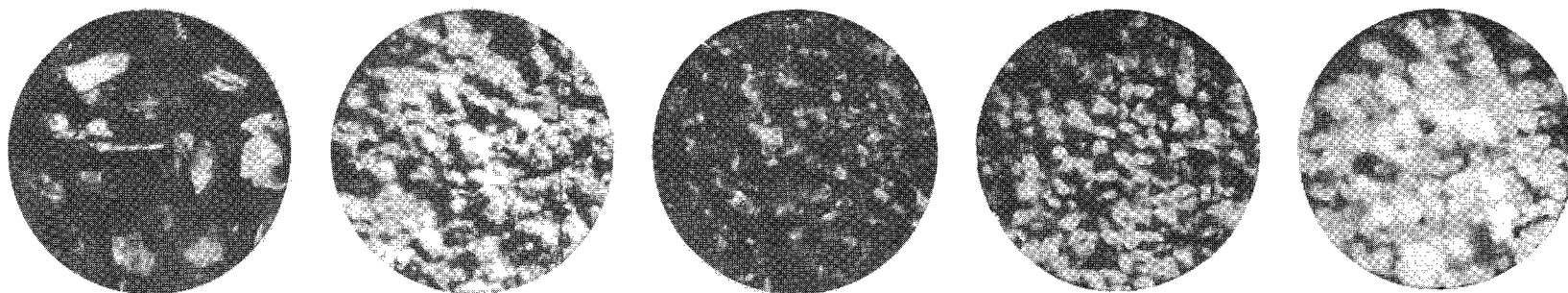


Figure 9.- Absolute spectral transmittance of quasi-microscope.



0.02° samples



0.04° samples

(a) Basalt.

(b) Limonite.

(c) Peridotite.

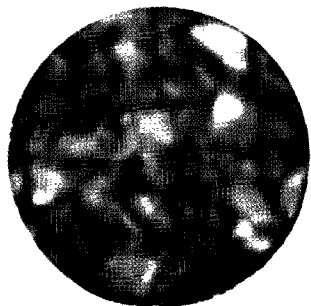
(d) Latite.

(e) Penacates 3.

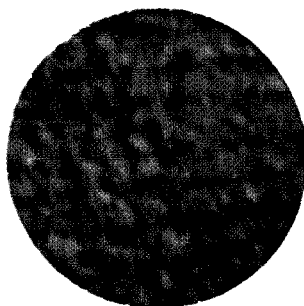
L-76-298

Figure 10.- Black and white images of geologic materials.

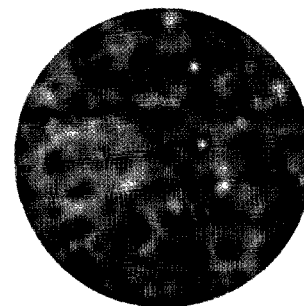




(a)



(b)



(c)

L-76-299

Figure 11.- Color images of geologic materials.

NATIONAL AERONAUTICS AND SPACE ADMINISTRATION  
WASHINGTON, D.C. 20546

OFFICIAL BUSINESS  
PENALTY FOR PRIVATE USE \$300

**SPECIAL FOURTH-CLASS RATE  
BOOK**

POSTAGE AND FEES PAID  
NATIONAL AERONAUTICS AND  
SPACE ADMINISTRATION  
451



017 001 C1 U D 770107 S00903DS  
DEPT OF THE AIR FORCE  
AF WEAPONS LABORATORY  
ATTN: TECHNICAL LIBRARY (SUL)  
KIRTLAND AFB NM 87117

POSTMASTER: If Undeliverable (Section 158  
Postal Manual) Do Not Return

*"The aeronautical and space activities of the United States shall be conducted so as to contribute . . . to the expansion of human knowledge of phenomena in the atmosphere and space. The Administration shall provide for the widest practicable and appropriate dissemination of information concerning its activities and the results thereof."*

—NATIONAL AERONAUTICS AND SPACE ACT OF 1958

## NASA SCIENTIFIC AND TECHNICAL PUBLICATIONS

**TECHNICAL REPORTS:** Scientific and technical information considered important, complete, and a lasting contribution to existing knowledge.

**TECHNICAL NOTES:** Information less broad in scope but nevertheless of importance as a contribution to existing knowledge.

**TECHNICAL MEMORANDUMS:** Information receiving limited distribution because of preliminary data, security classification, or other reasons. Also includes conference proceedings with either limited or unlimited distribution.

**CONTRACTOR REPORTS:** Scientific and technical information generated under a NASA contract or grant and considered an important contribution to existing knowledge.

**TECHNICAL TRANSLATIONS:** Information published in a foreign language considered to merit NASA distribution in English.

**SPECIAL PUBLICATIONS:** Information derived from or of value to NASA activities. Publications include final reports of major projects, monographs, data compilations, handbooks, sourcebooks, and special bibliographies.

**TECHNOLOGY UTILIZATION PUBLICATIONS:** Information on technology used by NASA that may be of particular interest in commercial and other non-aerospace applications. Publications include Tech Briefs, Technology Utilization Reports and Technology Surveys.

*Details on the availability of these publications may be obtained from:*

**SCIENTIFIC AND TECHNICAL INFORMATION OFFICE**

**NATIONAL AERONAUTICS AND SPACE ADMINISTRATION**  
Washington, D.C. 20546